Langmuir
Article
pubs.acs.org/Langmuir

Robust Fe_3O_4/SiO_2-Pt/Au/Pd Magnetic Nanocatalysts with Multifunctional Hyperbranched Polyglycerol Amplifiers

Li Zhou,[†,‡] Chao Gao,*[,‡] and Weijian Xu*[,†]

[†]*Institute of Polymer Science and Engineering, College of Chemistry and Chemical Engineering, Hunan University, Changsha 410082, P. R. China, and* [‡]*MOE Key Laboratory of Macromolecular Synthesis and Functionalization, Department of Polymer Science and Engineering, Zhejiang University, 38 Zheda Road, Hangzhou 310027, P. R. China*

Received February 5, 2010. Revised Manuscript Received April 1, 2010

Here we report a facile approach to prepare multicarboxylic hyperbranched polyglycerol (HPG)-grafted SiO_2-coated iron oxide (Fe_3O_4/SiO_2) magnetic hybrid support. This support combined the both features of Fe_3O_4 and HPG, facile magnetic separation, and favorable molecular structure with numerous functional groups. With the use of the grafted-HPGs as templates, various noble metal nanocatalysts such as Pt, Au, and Pd were directly grown on the surfaces of magnetic support with ultrasmall and nearly monodisperse sizes (e.g., the average sizes of Pt, Au, and Pd are 4.8 ± 0.5, 6.0 ± 0.6, and 4.0 ± 0.4 nm, respectively) and high coverage densities. Because of the amplification effect of HPG, high loading capacities of the nanocatalysts, around 0.296, 0.243, and 0.268 mmol/g for Pt, Au, and Pd, respectively, were achieved. Representative catalytic reactions including reduction of 4-nitrophenol, alcohol oxidation, and Heck reaction demonstrated the high catalytic activity of the noble metal nanocatalysts. Because of the stabilization of HPG templates, the nanocatalysts can be readily recycled by a magnet and reused for the next reactions with high efficiencies. The robust multifunctional magnetic hybrids will find important applications in catalysis and other fields such as drug delivery and bioseparations.

Introduction

With the development of nanoscience and nanotechnology, the combination of different nanomaterials to afford a multifunctional integrated nanosystem that simultaneously possesses optical, catalytic, electronic, and magnetic properties becomes possible.[1,2] This kind of nanosystem is significantly fascinating because of its potential applications in biomedicine, optical devices, and catalysis.[3−5]

For catalysis, it is well-known that homogeneous catalysts show higher catalytic activities than their heterogeneous counterparts because they can dissolve in reaction media making all catalytic sites accessible to the substrate.[6,7] However, the expensive noble metal catalysts are difficult to be recycled and thus cause huge waste and also contaminate the products. In practical industrial applications, homogeneous catalysis has a share of less than 20%, significantly lower than that of heterogeneous catalysis.[8] Therefore, the high catalytic activity is not the sole factor for an excellent catalyst, but a recyclable system in which the catalyst can be easily separated from the products and recycled through a separate rejuvenation procedure is also needed. On the other hand, for heterogeneous catalysis, the noble metal catalyst with nanoscale size and large surface areas immobilized on an appropriate support can also show comparable catalytic efficiency of the homogeneous catalyst to some extent.[9,10] Recently, immobilizing noble metal nanocatalysts on Fe_3O_4 magnetic support has drawn a great deal of attention due to the facile recycle process of the catalyst by an external magnetic field.[11−13] In addition, the Fe_3O_4 particles can be easily produced through precipitation of ferrite with the basic solution. Considering the Fe_3O_4 particles are reactive especially in an acid environment and thereby to lose their magnetic properties, silica as a protecting shell was usually utilized to coat the Fe_3O_4 particles to form a core−shell (Fe_3O_4/SiO_2) structure.[14] Meanwhile, the silica shell can prevent the aggregation of the Fe_3O_4 particles and provide numerous surface Si−OH groups for further modification.[15]

The metal nanocatalysts can be immobilized on the magnetic support through two approaches. The one is to deposit the presynthesized metal nanoparticles onto the support by chemical adsorption.[16,17] This approach allows the fine control over the size and shape of the metal nanoparticles, but the whole operation-steps are tedious; and moreover, the adsorbed nanocatalysts are

*To whom correspondence should be addressed. E-mail: chaogao@zju.edu.cn (C.G.); weijxu@hnu.cn (W.X.).

(1) Shevchenko, E. V.; Talapin, D. V.; Murray, C. B.; O'Brien, S. *J. Am. Chem. Soc.* **2006**, *128*, 3620–3637.
(2) Redl, F. X.; Cho, K. S.; Murray, C. B.; O'Brien, S. *Nature* **2003**, *423*, 968–971.
(3) Quarta, A.; Di-Corato, R.; Manna, L.; Argentiere, S.; Cingolani, R.; Barbarella, G.; Pellegrino, T. *J. Am. Chem. Soc.* **2008**, *130*, 10545–10555.
(4) Barbic, M. *Nano Lett.* **2005**, *5*, 187–190.
(5) Gao, X.; Yu, K. M. K.; Tam, K. Y.; Tsang, S. C. *Chem. Commun.* **2003**, 2998–2999.
(6) Corma, A.; Garcia, H. *Adv. Synth. Catal.* **2006**, *348*, 1391–1412.
(7) Widegren, J. A.; Finke, R. G. *J. Mol. Catal. A: Chem.* **2003**, *198*, 317–341.
(8) Stevens, P. D.; Li, G. F.; Fan, J. D.; Yen, M.; Gao, Y. *Chem. Commun.* **2005**, 4435–4437.
(9) Phan, N. T. S.; Jones, C. W. *J. Mol. Catal. A: Chem.* **2006**, *253*, 123–131.
(10) Thomas, J. M.; Johnson, B. F. G.; Raja, R.; Sankar, G.; Midgley, P. A. *Acc. Chem. Res.* **2003**, *36*, 20–30.
(11) Zhu, Y. H.; Peng, S. C.; Emi, A .; Zhenshun., S.; Monalisa.; Kemp, R. A. *Adv. Synth. Catal.* **2007**, *349*, 1917–1922.
(12) Liu, J. M.; Peng, X. G.; Sun, W.; Zhao, Y. W.; Xia, C. G. *Org. Lett.* **2008**, *10*, 3933–3936.
(13) Ding, S. J.; Xing, Y. C.; Radosz, M.; Shen, Y. Q. *Macromolecules* **2006**, *39*, 6399–6405.
(14) Deng, Y. H.; Wang, C. C.; Hu, J. H.; Yang, W. L.; Fu, S. K. *Colloids Surf. A* **2005**, *262*, 87–93.
(15) Morel, A. L.; Nikitenko, S. I.; Gionnet, K.; Wattiaux, A.; Lai-Kee-Him, J.; Labrugere, C.; Chevalier, B.; Deleris, G.; Petibois, C.; Brisson, A.; Simonoff, M. *ACS Nano* **2008**, *2*, 847–856.
(16) Ge, J. P.; Huynh, T.; Hu, Y. P.; Yin, Y. D. *Nano Lett.* **2008**, *8*, 931–934.
(17) Wang, Z. F.; Xiao, P. F.; Shen, B.; He, N. Y. *Colloids Surf. A* **2006**, *276*, 116–121.

Scheme 1. Process for Preparation of Noble Metal Nanocrystals (NCs) Supported on Hyperbranched Polyglycerol-Functionalized Magnetic Hybrids

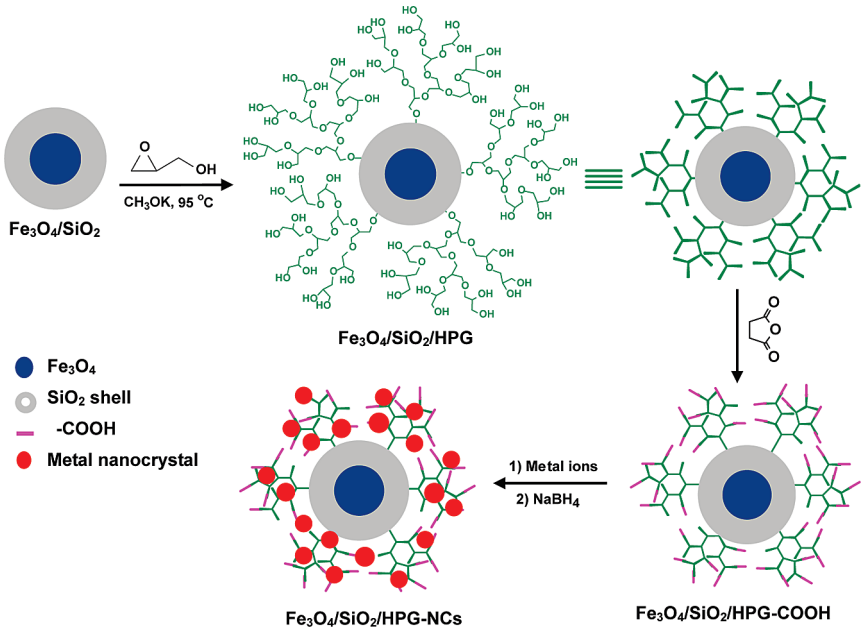

easy to be leached from the magnetic support during the catalytic reaction. The other is to directly grow metal nanoparticles on the magnetic support using the pregrafted organic functional molecules or polymers as a stabilizer.[18,19] This protocol is facile to conduct, but the size of metal catalyst is hard to be controlled, and more awfully, the amount of catalyst on the magnetic support is relatively small. This is because the support surfaces lack the organic components with sufficient functional groups and favorable molecular structure for the growth and stabilization of metal nanoparticles. To overcome this limitation, polyamidoamine (PAMAM) dendrimer with a well-defined structure and numerous interior tertiary amine and terminal amino groups was first considered to graft from the Fe_3O_4 supports. Therein, PAMAM can act as structurally and chemically well-defined templates and robust stabilizer for preparing metal nanoparticles, and this was systematically studied by the groups of Crooks and Esumi.[20−22] At the same time, the high catalytic activity of PAMAM-metal nanoparticles (e.g., PAMAM-Pd for hydrogenation, Heck reaction, and Suzuki reaction) was also demonstrated by the groups of Crooks and Christensen.[23−25] The groups of Alper and Gao successfully grafted the PAMAM from the surface of Fe_3O_4/SiO_2 and then used as a noble metal nanocatalyst support for selective hydroformylation and hydrogenation catalysis, respectively.[26,27] The results showed that such a magnetic particle-supported catalyst is highly selective and reactive. Although the PAMAM dendrimer possesses so many advantages, tedious operation steps and long synthetic periods, which do not meet the large-scale application in industry, are needed to graft the PAMAM from the Fe_3O_4/SiO_2 surface. In contrast to the dendrimers, hyperbranched polymers (HPs) which can be easily accessible have also been successfully used as templates for metal nanoparticles.[28−30] However, no report has been published on growing HPs on the magnetic particles to serve as a catalyst support yet.

In this article, we designed and synthesized hyperbranched polyglycerol (HPG)-functionalized magnetic Fe_3O_4/SiO_2 hybrids (Fe_3O_4/SiO_2/HPG) by surface-initiated ring-opening polymerization of glycidol to *in situ* growth of metal nanoparticles (see Scheme 1). The advantages of this strategy are as follows: (1) Fe_3O_4/SiO_2 magnetic nanoparticle as a catalyst support can facilitate its separation from the reaction media by a magnetic field. (2) HPG, a well-known biocompatible HP with numerous reactive hydroxyl groups, can be easily synthesized through only a one-step reaction under mild conditions, and thus the Fe_3O_4/SiO_2/HPG magnetic supports can be scalably and cost-effectively produced. (3) It is easy to transform the hydroxyl groups into carboxylic groups that are crucial for the nanocatalyst chelation and water solubilization of products. (4) The grafted HPGs are dendritic templates in which monodisperse noble metal nanoparticles can be readily fabricated by *in situ* reduction of the corresponding ions. (5) HPG with a high density of hydroxyl or carboxylic acid groups can play the role of a functional amplifier, which can significantly increase the loading capacity of the metal nanoparticles and improve the catalysis power accordingly. Moreover, the catalytic activities of the resulting magnetic nanocatalysts were evaluated by three classic reactions including reduction of 4-nitrophenol, alcohol oxidation, and Heck reaction.

(18) Chang, Y. C.; Chen, D. H. *J. Hazard. Mater*. **2009**, *165*, 664–669.
(19) Yi, D. K.; Lee, S. S.; Ying, J. Y. *Chem. Mater*. **2006**, *18*, 2459–2461.
(20) Crooks, R. M.; Zhao, M. Q.; Sun, L.; Chechik, V.; Yeung, L. K. *Acc. Chem. Res*. **2001**, *34*, 181–190.
(21) Scott, R. W. J.; Wilson, O. M.; Crooks, R. M. *J. Phys. Chem. B* **2005**, *109*, 692–704.
(22) Esumi, K.; Isono, R.; Yoshimura, T. *Langmuir* **2004**, *20*, 237–243.
(23) Wilson, O. M.; Knecht, M. R.; Garcia-Martinez, J. C.; Crooks, R. M. *J. Am. Chem. Soc*. **2006**, *128*, 4510–4511.
(24) Rahim, E. H.; Kamounah, F. S.; Frederiksen, J.; Christensen, J. B. *Nano Lett*. **2001**, *1*, 499–501.
(25) Pittelkow, M.; Moth-Poulsen, K.; Boas, U.; Christensen, J. B. *Langmuir* **2003**, *19*, 7682–7684.
(26) Abu-Reziq, R.; Alper, H.; Wang, D. S.; Post, M. L. *J. Am. Chem. Soc*. **2006**, *128*, 5279–5282.
(27) Jiang, Y. J.; Jiang, J. H.; Gao, Q. M.; Ruan, M. L.; Yu, H. M.; Qi, L. J. *Nanotechnology* **2008**, *19*, 075714.
(28) Tabuani, D.; Monticelli, O.; Chincarini, A.; Bianchini, C.; Vizza, F.; Moneti, S.; Russo, S. *Macromolecules* **2003**, *36*, 4294–4301.
(29) Schlotterbeck, U.; Aymonier, C.; Thomann, R.; Hofmeister, H.; Tromp, M.; Richtering, W.; Mecking, S. *Adv. Funct. Mater*. **2004**, *14*, 999–1004.
(30) Pérignon, N.; Mingotaud, A. F.; Marty, J. D.; Rico-Lattes, I.; Mingotaud, C. *Chem. Mater*. **2004**, *16*, 4856–4858.

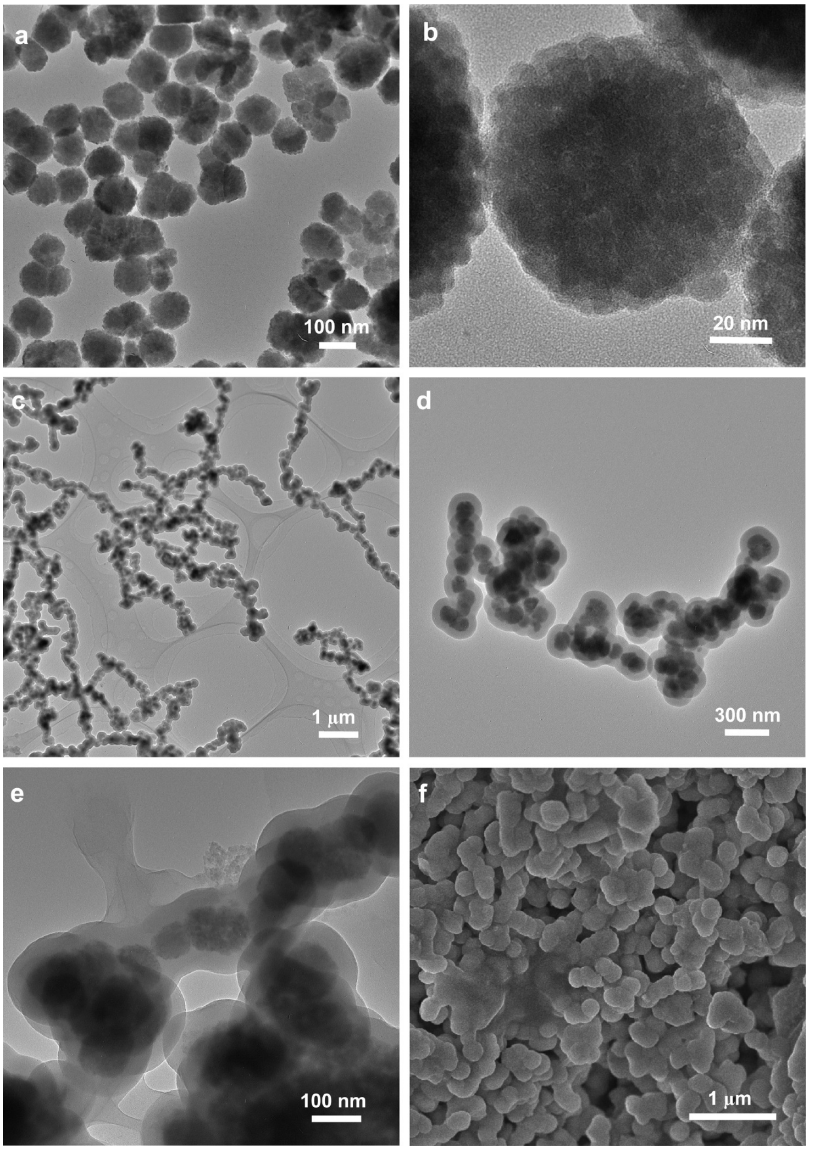

Figure 1. TEM images of Fe_3O_4 at low (a) and high (b) magnification, Fe_3O_4/SiO_2 at low (c) and high (d) magnification, and Fe_3O_4/SiO_2/HPG (e). SEM image of Fe_3O_4/SiO_2/HPG (f).

Experimental Section

Materials. Potassium tetrachloroplatinate (K_2PtCl_4), palladium nitrate dihydrate based ($Pd(NO_3)_2 \cdot 2H_2O$), chloroauric acid tetrahydrate ($HAuCl_4 \cdot 4H_2O$), sodium borohydride ($NaBH_4$), tetraethyl orthosilicate (TEOS), rhodamine B, iron(III) chloride ($FeCl_3$) powder, iron(II) chloride tetrahydrate ($FeCl_2 \cdot 4H_2O$), ammonia solution (25 wt %), potassium methylate solution in methanol (CH_3OK, 25 wt %), and glycidol (96%) were purchased from Sigma-Aldrich and used as received. *N*,*N*′-Dicyclohexylcarbodiimide (DCC) and 4-(dimethylamino) pyridine (DMAP) were purchased from GL Biochem Ltd. (Shanghai, China). Dioxane and tetrahydrofuran (THF) were freshly distilled in the presence of calcium hydride before each polymerization. All other reagents were of analytical grade and used as received without further purification.

Synthesis. (1) Fe_3O_4 particles were prepared according to the literature,[31] and subsequently Fe_3O_4 nanoparticles were coated with silica (Fe_3O_4/SiO_2) through the Stöber method.[32] In a typical procedure, the suspension of the as-prepared Fe_3O_4 (0.5 g) nanoparticles was diluted by a mixture of ethanol (50 mL) and water (9 mL). After addition of 1 mL of ammonia solution (25 wt %), 0.5 mL of TEOS was added to the reaction solution with mechanical stirring at room temperature for 16 h. The resulting Fe_3O_4/SiO_2 particles were washed by deionized water and methanol to eliminate excess reactants and then collected by an external magnet. Finally, the Fe_3O_4/SiO_2 particles were dried in a vacuum oven at 90 °C for 24 h. (2) Hyperbranched polyglycerol-functionalized Fe_3O_4/SiO_2 particles (Fe_3O_4/SiO_2/HPG):[33−35] typically, Fe_3O_4/SiO_2 nanoparticles (100 mg) were mixed with 28 μL (0.938 mmol) of potassium methylate (CH_3OK) solution and 2.5 mL of anhydrous tetrahydrofuran (THF) in a flask. The mixture was stirred for 1 h, before which excess methanol was removed by vacuum. Then 10 mL of anhydrous dioxane was added, and the flask was kept in an oil bath at 95 °C. Glycidol (2.0 g, 27.04 mmol) was added dropwise over a period of 15 h. After completion of the monomer addition, the mixture was stirred for an additional 1 h. The mixture was quenched and dispersed in methanol and subsequently separated by a magnet

(31) Shao, D. D.; Xu, K. K.; Song, X. J.; Hu, J. H.; Yang, W. L.; Wang, C. C. *J. Colloid Interface Sci.* **2009**, *336*, 526–532.
(32) Stöber, W.; Fink, A.; Bohn, E. *J. Colloid Interface Sci.* **1968**, *26*, 62–69.
(33) Kan, M.; Huck, W. T. S. *Macromolecules* **2003**, *36*, 5088–5093.
(34) Zhou, L.; Gao, C.; Xu, W. J. *Macromol. Chem. Phys.* **2009**, *210*, 1011–1018.
(35) Zhou, L.; Gao, C.; Xu, W. J.; Wang, X.; Xu, Y. H. *Biomacromolecules* **2009**, *10*, 1865–1874.

and washed with methanol. After repeated washing and separation steps, the resulting solid was dried overnight in a vacuum, yielding 143 mg of Fe_3O_4/SiO_2/HPG hybrids. (3) Rhodamine B-conjugated Fe_3O_4/SiO_2/HPG by DCC coupling chemistry: typically, Fe_3O_4/SiO_2/HPG (50 mg), rhodamine B (10 mg, 0.02 mmol), and 5 mL of *N*,*N*-dimethylformamide (DMF) were placed in a dry flask and treated in an ultrasonic bath for 3 min. Then, DCC (50 mg) and DMAP (15 mg) were added to the flask, and the mixture was stirred at 80 °C for 24 h. The product (designed as Fe_3O_4/SiO_2/HPG-RB) was separated by a magnet and washed with ethanol repeatedly until the washed ethanol became colorless. (4) Fe_3O_4/SiO_2/HPG-COOH hybrids: typically, Fe_3O_4/SiO_2/HPG (100 mg), triethylamine (100 mg), and succinic anhydride (80 mg) were dispersed in 10 mL of DMF in a flask. The mixture was stirred at 60 °C for 4 h before the resulting solids were separated by a magnet and washed with methanol. (5) Noble metal nanocrystals supported on Fe_3O_4/SiO_2/HPG-COOH particles: typically, 12 mg of K_2PtCl_4, $HAuCl_4$, or $Pd(NO_3)_2$ aqueous solution and Fe_3O_4/SiO_2/HPG-COOH (30 mg) was mixed in 10 mL of deionized water and stirred at room temperature for 1 h. After that, the solid was separated by a magnet and washed with deionized water. This magnetic separation and wash process was repeated three times. With determination of the concentrations of metal ions in solution before and after the adsorption process using an atomic absorption spectrometer (WARIAN AA240), the loading amounts of salts are calculated to be 0.315, 0.254, and 0.291 mmol/g for K_2PtCl_4, $HAuCl_4$, and $Pd(NO_3)_2$, respectively. Then, the resulting solid was redispersed in deionized water, and 0.2 mL of freshly prepared $NaBH_4$ (0.25 M) aqueous solution was added and stirred for 30 min. Finally, the product was collected by a magnet and washed with deionized water. This magnetic separation and wash process was repeated at least three times. On the basis of the results obtained from the measurements of the atomic absorption spectrometer, the loading amounts of the noble metal nanoparticles on Fe_3O_4/SiO_2/HPG-COOH are calculated to be 0.296 mmol of Pt/g, 0.243 mmol of Au/g, and 0.268 mmol of Pd/g, respectively. This indicates that the conversions of the loaded salts to their corresponding nanoparticles are 94%, 95.7%, and 92.1% for Pt, Pd, and Au, respectively. For comparison, Fe_3O_4/SiO_2-NH_2 (TGA weight loss, 5.4 wt % between 200 and 500 °C; -NH_2, 0.93 mmol/g) was prepared according to the literature and also used as support for the Pt catalyst (Pt, 0. 053 mmol/g).[36]

Catalysis. (1) Reduction of 4-nitrophenol: typically, in a standard quartz cuvette, 4-nitrophenol (0.025 mL, 0.01 M), $NaBH_4$ (0.1 mL, 0.1 M), and deionized water (2.2 mL) were added. After addition of Fe_3O_4/SiO_2/HPG-Pt (7 mg) (or Fe_3O_4/SiO_2-NH_2-Pt) catalyst, the bright yellow solution gradually fades as the reaction progresses. UV−vis spectra were monitored in the sequence of time. After the catalytic reaction, the Fe_3O_4/SiO_2/HPG-Pt catalyst was collected by a magnet and washed with ethanol. Then, the recovered catalyst was reused to initiate another cycle of reaction. The same procedures were conducted for at least 10 cycles. (2) Alcohol oxidation: the selective aerobic oxidation of alcohols was performed in a test tube under stirring. For a typical run, the reaction was carried out with 16 mg of benzyl alcohol (0.15 mmol), 62 mg of K_2CO_3 (0.45 mmol, 3 equiv), 10 mL of deionized water, and 18.5 mg of Fe_3O_4/SiO_2/HPG-Au catalyst at 310 K. The reaction mixture was sampled at fixed intervals, quenched with 1.0 M HCl, and extracted with ethyl acetate. The extracted organic layer was dried over Na_2SO_4 and subsequently analyzed by gas chromatography (GC, Aglient, 6890N). (3) Heck coupling reaction: typically, to a test tube, aryl halid (0.1 mmol), olefin (0.2 mmol, 2 equiv), NaOAc (0.18 mmol, 1.8 equiv), Fe_3O_4/SiO_2/HPG-Pd (11.4 mg) catalyst, and 8 mL of DMF were added, and the mixture was stirred at 140 °C. After the reaction, the mixture was cooled to room temperature and extracted with toluene. The organic layer was washed with water and dried and then analyzed by gas chromatography (GC).

(36) Zhou, L.; Gao, C.; Xu, W. J. *J. Mater. Chem.* **2009**, *19*, 5655–5664.

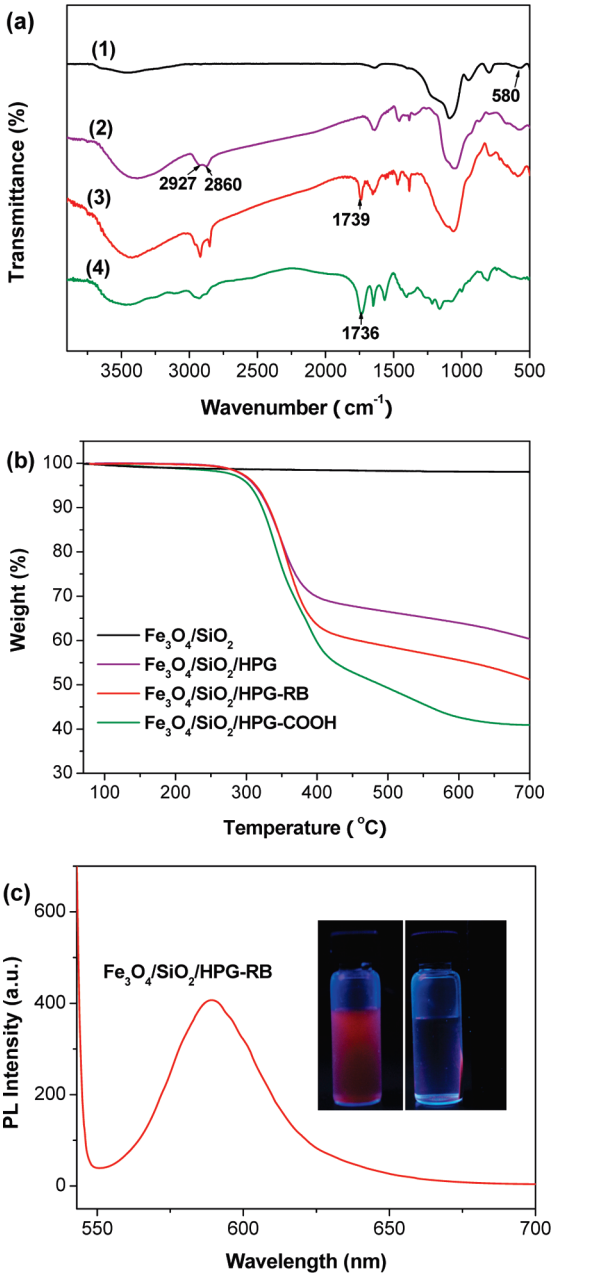

Figure 2. (a) FT-IR spectra of Fe_3O_4/SiO_2 (1), Fe_3O_4/SiO_2/HPG (2), Fe_3O_4/SiO_2/HPG-RB (3), and Fe_3O_4/SiO_2/HPG-COOH (4). (b) TGA curves of Fe_3O_4/SiO_2, Fe_3O_4/SiO_2/HPG, Fe_3O_4/SiO_2/HPG-RB, and Fe_3O_4/SiO_2/HPG-COOH. (c) Emission spectrum of Fe_3O_4/SiO_2/HPG-RB, λex = 540 nm. The inserts show the photographs of aqueous Fe_3O_4/SiO_2/HPG-RB under excitation of 365 nm before (left) and after (right) using an external magnet.

Characterization. Thermogravimetric analysis (TGA) was carried on a Perkin-Elmer (PE) TGA-7 instrument with a heating rate of 20 °C min^{-1} in a nitrogen flow (20 mL min^{-1}). Absorption spectra were recorded at room temperature on a PE Lambda 20 UV−visible spectrometer. Fourier transform-infrared (FT-IR) spectra were recorded using a PE Paragon 1000 spectrometer (KBr disk). X-ray powder diffraction (XRD) spectra were taken on a Bruker AXS D8-advance X-ray diffractometer with Cu Kα radiation. The magnetic moment was recorded at 300 K on a JPMS-9H-EVERCOOL (QD) vibrating-sample magnetometer (VSM). Transmission electron microscopy (TEM) studies were performed on a JEOL JEL2010 electron microscope at 200 kV. Scanning electron microscopy (SEM) images and energy dispersive

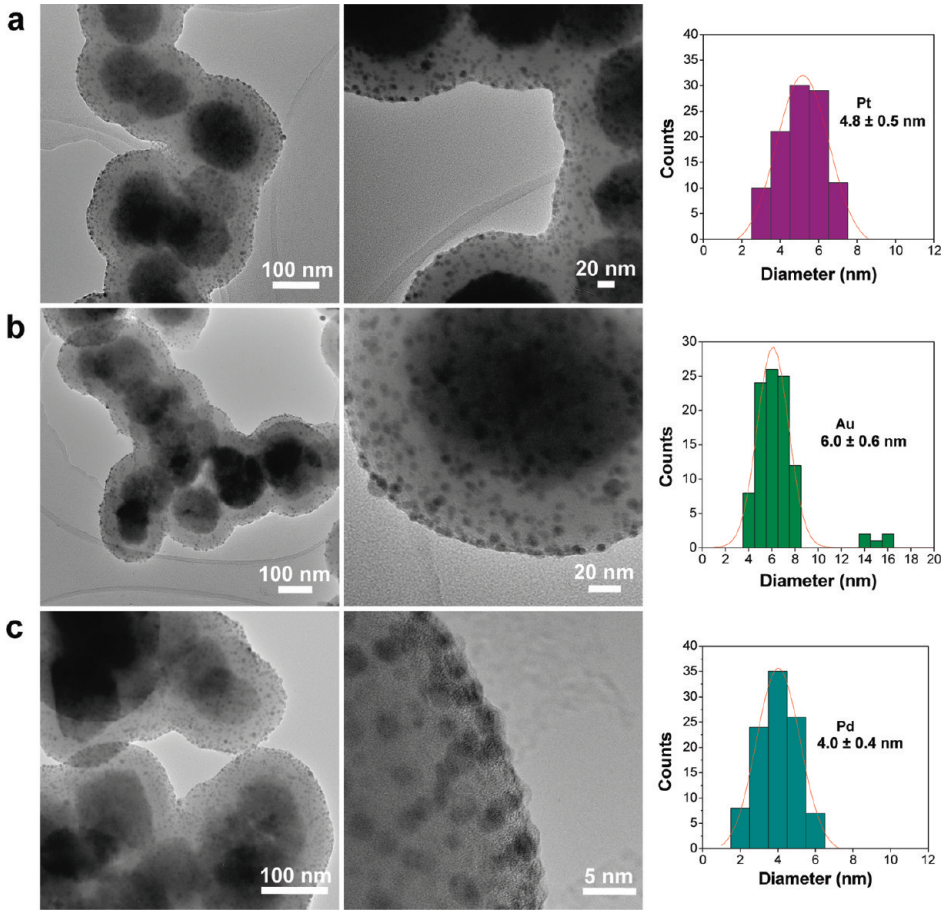

Figure 3. TEM images and the size distributions of Pt (a), Au (b), and Pd (c) nanoparticles on the Fe_3O_4/SiO_2/HPG-COOH supports. A total of 150 particles were measured to get the size distribution.

X-ray (EDX) spectra were recorded using a FEISIRION 200 field-emission microscope.

Results and Discussion

Synthesis, Functionalization, and Morphology of Fe_3O_4/SiO_2/HPG. The Fe_3O_4 magnetic particles with an average diameter of 98 nm (see Figure 1a,b) were prepared by precipitation of iron(II) ions in basic solution.[31] Each of the particles was composed of a lot of small Fe_3O_4 nanoparticles with a size around 10 nm. So the Fe_3O_4 particles show superparamagnetic property at room temperature and its saturation magnetic moment is 62 emu/g (see Figure S1 in the Supporting Information). Subsequently, silica was coated on the Fe_3O_4 to form Fe_3O_4/SiO_2 core−shell particles (Figure 1c,d) through hydrolysis of tetraethyl orthosilicate (TEOS) according to the Stöber method.[32] This coating reaction is indispensable for two reasons. First, the SiO_2 shell can effectively prevent the aggregation and chemical degradation of the Fe_3O_4 nanoparticles in a harsh liquid environment. Second, the surface Si−OH groups can be utilized to directly initiate the ring-opening polymerization of glycidol, affording HPG-grafted magnetic particles (Fe_3O_4/SiO_2/HPG).[33] The reactions were monitored by FT-IR spectra and TGA, as shown in Figure 2a,b. From Figure 2a, for Fe_3O_4/SiO_2, the bands at 580 and 1100 cm^{-1} were assigned to the vibration of the Fe−O and Si−O bonds, respectively, demonstrating the existence of Fe_3O_4 and SiO_2 components. After the polymerization, two obvious bands at 2860 and 2927 cm^{-1} associated with C−H stretching appeared. This is in accordance with the predicted structure of Fe_3O_4/SiO_2/HPG. From the TGA curves, only 2 wt % of weight loss was found for Fe_3O_4/SiO_2 below 700 °C. While after the polymerization, 33.2 wt % of weight loss was detected between 200 and 500 °C, suggesting the successful grafting of HPG from the surface of Fe_3O_4/SiO_2. Correspondingly, the hydroxyl density of the functionalized magnetic hybrid is calculated to be ~4.49 mmol/g. Such a high content of hydroxyl groups is attributed to the amplification effect of the HP that tens to hundreds of hydroxyl groups resulted from one Si−OH group and can provide a convenient platform for further modification.[34,35] To show the versatility of the reactive platform of Fe_3O_4/SiO_2/HPG, fluorescent rhodamine B (RB) was conjugated onto Fe_3O_4/SiO_2/HPG by one-step *N*,*N*′-dicyclohexylcarbodiimide (DCC) coupling, affording bifunctional hybrids (Fe_3O_4/SiO_2/HPG-RB) with both fluorescent and magnetic properties. This reaction was confirmed by FT-IR and TGA characterizations (Figure 2a,b). The photoluminescence spectrum of Fe_3O_4/SiO_2/HPG-RB shows an obvious emission peak at 589 nm, and strong red fluorescence and magnetism were observed under UV light (Figure 2c). Furthermore, the surface hydroxyl groups can be readily transformed into carboxylic groups by the reaction with succinic anhydride for 4 h at 60 °C in the presence of triethylamine. This successful postfunctionalization was also confirmed by FT-IR and TGA measurements. For Fe_3O_4/SiO_2/HPG-COOH, a new band of carbonyl groups at 1736 cm^{-1} appeared in the FT-IR spectrum (Figure 2a), and its weight loss between 200 and 500 °C increased to 50.6 wt % (Figure 2b), corresponding to the density of 2.61 mmol/g of carboxylic groups on the periphery of Fe_3O_4/SiO_2.

The morphology of Fe_3O_4/SiO_2/HPG was observed by transmission electron microscopy (TEM) and scanning electron microscopy

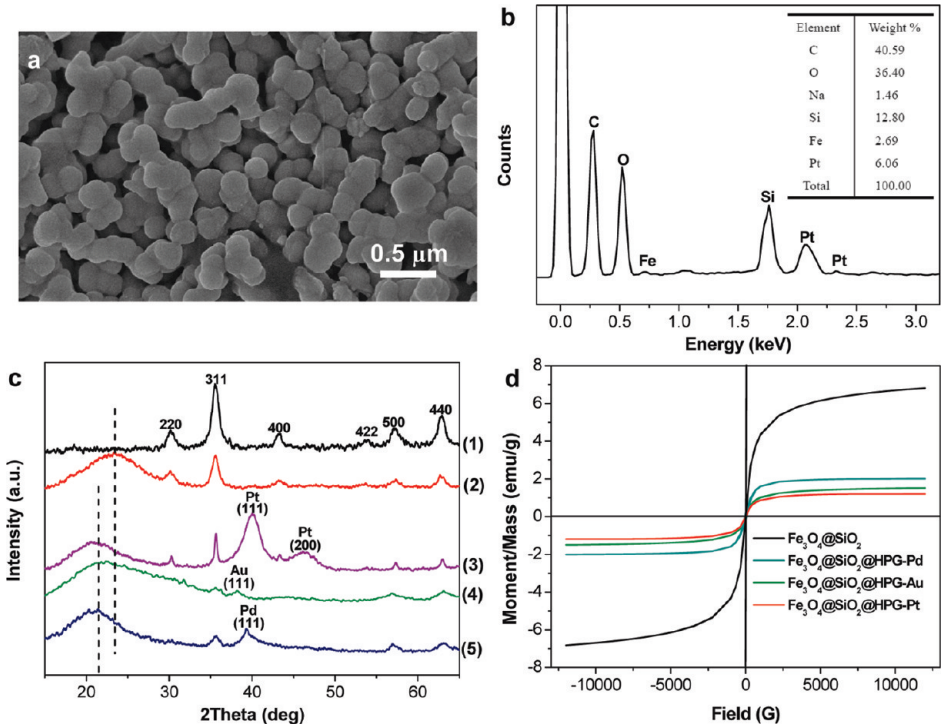

Figure 4. SEM image (a) of Fe_3O_4/SiO_2/HPG-Pt and its corresponding EDX spectrum (b). (c) Powder XRD patterns of Fe_3O_4 (1), Fe_3O_4/SiO_2 (2), Fe_3O_4/SiO_2/HPG-Pt (3), Fe_3O_4/SiO_2/HPG-Au (4), and Fe_3O_4/SiO_2/HPG-Pd (5). (d) Magnetization curves at 300 K for Fe_3O_4/SiO_2, Fe_3O_4/SiO_2/HPG-Pt, Fe_3O_4/SiO_2/HPG-Au, and Fe_3O_4/SiO_2/HPG-Pd.

(SEM) (Figure 1e,f). Owing to the low contrast, the HPG shell confirmed by FT-IR and TGA could hardly be detected by TEM. Nevertheless, a continuous phase of HPG can be observed from the SEM image.

Magnetic Hybrids of Fe_3O_4/SiO_2/HPG-Pt/Au/Pd. Because of the high density of carboxylic groups derived from HPG on the surface of magnetic hybrids, various noble metal ions such as Pt^{2+}, Au^{3+}, and Pd^{2+} can partition into the HPG where they are strongly complexed by carboxylic groups. Subsequent chemical reduction of the HPG/metal ion complexes by $NaBH_4$ yields zerovalent metal nanocrystals that remain sterically trapped within the HPG, generating the anticipated magnetic nanocatalysts of Fe_3O_4/SiO_2/HPG-Pt/Au/Pd (see Scheme 1). There are many works on using functionalized-magnetic particles as the catalyst support; however, for the carboxylic magnetic support, rare reports can be found because tedious synthetic procedures are needed and moreover the grafted carboxylic density is too low to prepare a high content of metal nanocatalysts. Herein, HPG can act as a molecular amplifier that contains numerous carboxylic groups in a single HPG macromolecule. By determination of the concentration of metal ions in solution before and after the adsorption process with the atomic absorption spectrometer, the contents of Pt, Au, and Pd on the magnetic support are ~0.296, 0.243, and 0.268 mmol/g, respectively. These values are much higher than that of the amino silane-coupling agent modified Fe_3O_4/SiO_2 (Fe_3O_4/SiO_2-NH_2) support reported by others (for Pd, 0.075 mmol/g) and ourselves (for Pt, 0.053 mmol/g), and even higher than the PAMAM dendrimer-grafted Fe_3O_4/SiO_2 (for Pd, 0.246 mmol/g).[17,27] Such a loading record is mainly ascribed to both the functional amplification effect of dendritic macromolecules and the irregularly branched structure of HPs. Because of the steric hindrance (or umbrella effect) of external units to the internal of a dendrimer, the effective functional groups for complexing of ions becomes less than those of a hyperbranched analogue. Considering two carboxylic groups are needed for complexing Pt^{2+} or Pd^{2+} and three carboxylic groups for Au^{3+}, the participants of carboxylic groups for growing metal nanoparticles of Pt, Au, and Pd are as high as 23%, 28%, and 21%, respectively.

The morphology and sizes of the metal particles was observed by TEM as shown in Figure 3 (also see Figure S3−S5 in the Supporting Information). As we can see, the as-prepared metal nanoparticles are spherical without obvious aggregation. The sizes of Pt, Au, and Pd particles are uniform, and the mean diameters of Pt, Au, and Pd are 4.8 ± 0.5, 6.0 ± 0.6, and 4.0 ± 0.4 nm, respectively. All these indicate that the HPG-COOH can serve as a versatile platform to first adsorb metal ions and then stabilize the as-prepared metal nanoparticles.

The morphology of Fe_3O_4/SiO_2/HPG-metal nanoparticle hybrids was also observed by SEM (Figure 4a, also see Figure S6a,c in the Supporting Information). There is no obvious change for the Fe_3O_4/SiO_2/HPG before and after the *in situ* growth of metal nanoparticles. The corresponding energy dispersive X-ray (EDX) spectra demonstrated the existence of C, O, Si, Fe, and Pt (see Figure S6b,d in the Supporting Information for other samples) elements, of which the elements of Fe arises from Fe_3O_4, the elements of C and Si arise from HPG and SiO_2, and the elements of Pt arises from the Pt nanoparticles (Figure 4b). The content of Pt according to the EDX results is ~0.311 mmol/g (6.06 wt %), which is very close to the value of 0.296 mmol/g obtained from the atom-absorption spectrometer technique, further demonstrating the high loading capacity of the Pt nanoparticles for the magnetic support. Similar results were also observed for Fe_3O_4/SiO_2/HPG-Au (according to EDX results, 0.336 mmol/g) and Fe_3O_4/SiO_2/HPG-Pd (according to EDX results, 0.454 mmol/g) (Figure S6b,d in the Supporting Information), corroborating the generality and the amplification effect of the versatile magnetic platform of Fe_3O_4/SiO_2/HPG for growing noble metal nanocrystals.

The crystalline structures of the pristine Fe_3O_4 particles and magnetic hybrids were determined by powder X-ray diffraction

(XRD). As presented in Figure 4c, six characteristic diffraction peaks (2θ = 30.1°, 35.5°, 43.3°, 53.5°, 57.3°, and 62.7°) can be clearly observed for Fe_3O_4 particles, indicating their well crystallized structure. After coating by SiO_2, a new broad peak around 23° appeared because of the existence of amorphous silica. For Fe_3O_4/SiO_2/HPG-metal nanoparticle hybrids, the broad peak was transferred to 21° due to the synergetic effect of amorphous silica and HPG polymer. Moreover, new peaks corresponding to the (111) reflection of Pt, Au, and Pd crystal were observed for Fe_3O_4/SiO_2/HPG-Pt, Fe_3O_4/SiO_2/HPG-Au, and Fe_3O_4/SiO_2/HPG-Pd, respectively, confirming the successful growth of metal particles on the surface of magnetic hybrids again.

The magnetic properties of the hybrids containing a magnetite component were studied by a vibrating sample magnetometer (VSM) at 300 K (Figure 4d). The magnetization curves show that all the samples are superparamagnetic at room temperature. The saturation magnetization values for Fe_3O_4/SiO_2, Fe_3O_4/SiO_2/HPG-Pt, Fe_3O_4/SiO_2/HPG-Au, and Fe_3O_4/SiO_2/HPG-Pd were 6.8, 1.2, 1.5, and 2.0 emu/g, respectively. These results indicated that the magnetization of hybrids decreased considerably with the increase of HPG polymer and metal nanoparticle components. Nevertheless, the magnetic hybrid supported catalysts can still be separated to the sidewall of the reactor from the solution within 30 s using a magnet of 4000 Gs. This promises the facile magnetic separation for their practical application in catalysis.

Catalysis of Magnetic Nanocatalysts. To know whether the as-prepared magnetic nanocatalysts possess high catalytic activities, we first investigated the Fe_3O_4/SiO_2/HPG-Pt by the reduction of 4-nitrophenol in the presence of $NaBH_4$ at room temperature, which is a well-known model reaction and has been widely used to evaluate the catalytic rate of noble metal catalysts.[37,38] For comparison, Fe_3O_4/SiO_2-NH_2-Pt catalyst was also investigated under the same content of Pt catalyst. The reduction process was monitored by measuring the UV−vis spectra at different time (t) as shown in Figure 5a. In the absence of any catalysts, the characteristic peak at 400 nm ascribed to 4-nitrophenol remains unaltered even when a large excess of $NaBH_4$ was added. After the addition of Pt catalyst, the peak at 400 nm decreases gradually with time, while a new peak at 295 nm appears due to the formation of 4-aminophenol. Seen from the sample solution, the bright-yellow solution gradually becomes colorless after the addition of Fe_3O_4/SiO_2/HPG-Pt for 6 min or Fe_3O_4/SiO_2-NH_2-Pt for 15 min, indicating the complete reduction of 4-nitrophenol (see the insert of Figure 5c). Since the concentration of $NaBH_4$ greatly exceeded that of 4-nitrophenol and the Pt catalyst, the rates of the reduction are assumed to be independent of the concentration of 4-nitrophenol. Therefore, the kinetics of this reduction can be treated as pseudofirst-order to 4-nitrophenol concentration.[39] The kinetic equation of the reduction can be expressed as

$$\ln(A_t/A_0) = -k_{ap}t \quad (1)$$

where A_0 is the initial absorbance of 4-nitrophenol at 400 nm, A_t is the absorbance of 4-nitrophenol at 400 nm at time t, and k_{ap} is the apparent rate constant. The plot of ln (A_t/A_0) against t should give a straight line with slope $-k_{ap}$. As seen in Figure 5b, both Fe_3O_4/SiO_2/HPG-Pt and Fe_3O_4/SiO_2-NH_2-Pt show a straight line, indicating the good coincidence with the pseudofirst-order equation. On the basis of the plot, the k_{ap}s for Fe_3O_4/SiO_2/HPG-Pt and Fe_3O_4/SiO_2-NH_2-Pt are 0.0069 and 0.0021, respectively, suggesting that the Fe_3O_4/SiO_2/HPG-Pt possesses much higher catalytic activity and efficiency than the Fe_3O_4/SiO_2-NH_2-Pt. In addition, we found that the Fe_3O_4/SiO_2/HPG-Pt could still exhibit excellent catalytic activity even after 10 consecutive cycles of magnetic separation−reduction, while for Fe_3O_4/SiO_2-NH_2-Pt only 50% of catalytic efficiency was retained after 6 cycles and even was completely lost after 10 cycles (Figure 5c).

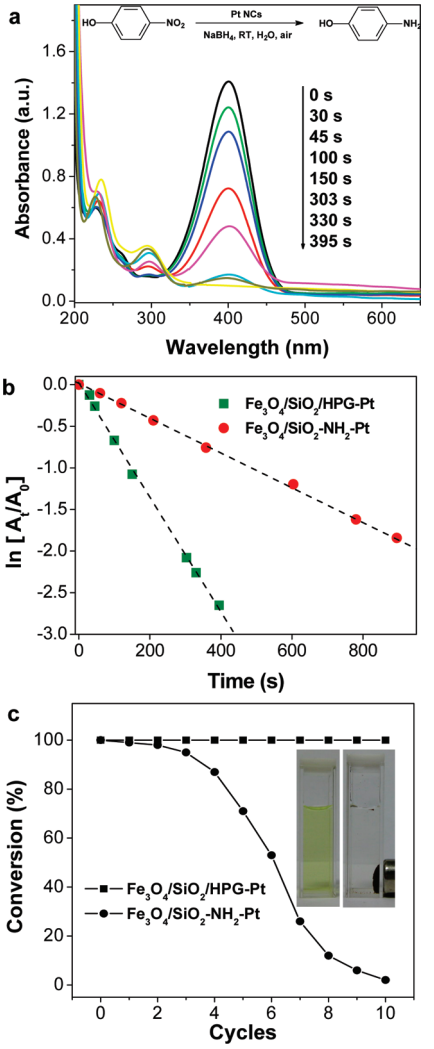

Figure 5. (a) UV−vis spectra showing the gradual reduction of 4-nitrophenol with Fe_3O_4/SiO_2/HPG-Pt catalyst. (b) Plots of ln[A_t/A_0] against time for the reduction of 4-nitrophenol with Fe_3O_4/SiO_2/HPG-Pt and Fe_3O_4/SiO_2-NH_2-Pt catalysts, respectively. (c) Conversion of 4-nitrophenol in 11 successive cycles of reduction and magnetic separation with Fe_3O_4/SiO_2/HPG-Pt and Fe_3O_4/SiO_2-NH_2-Pt catalysts, respectively. The inset shows the photographs of the 4-nitrophenol and $NaBH_4$ solution before adding Fe_3O_4/SiO_2/HPG-Pt catalysts (left) and magnetic separation of catalyst after the reaction (right).

To probe why the Pt nanoparticles supported on Fe_3O_4/SiO_2/HPG could show much better catalytic properties than on Fe_3O_4/SiO_2-NH_2, TEM observations were performed for the samples after catalysis reaction (Figure 6). As can be seen, the Pt nanoparticles were still uniformly distributed on the magnetic supports even after three cycles of reduction without showing obvious variation compared with the unused ones (Figure 6a,b). While on the Fe_3O_4/SiO_2-NH_2 support, the Pt particles with sizes of 3−10 nm were sparsely dispersed on its surface and showed obvious aggregation (Figure 6c). Furthermore, after three cycles

(37) Huang, T.; Meng, F.; Qi, L. M. *J. Phys. Chem. C* **2009**, *113*, 13636–13642.
(38) Jana, S.; Ghosh, S. K.; Nath, S.; Pande, S.; Praharaj, S.; Panigrahi, S.; Basu, S.; Endo, T.; Pal, T. *Appl. Catal., A: Gen.* **2006**, *313*, 41–48.
(39) Mei, Y.; Lu, Y.; Polzer, F.; Ballauff, M.; Drechsler, M. *Chem. Mater.* **2007**, *19*, 1062–1069.

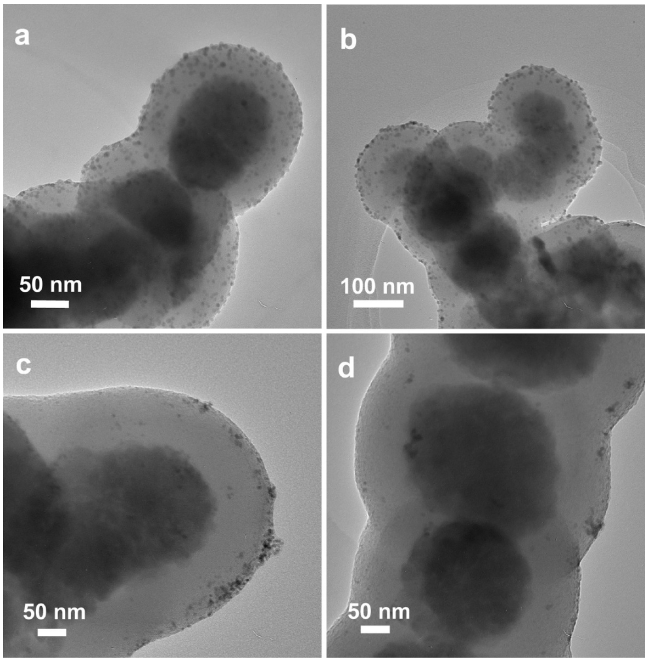

Figure 6. TEM images of Fe_3O_4/SiO_2/HPG-Pt catalyst after three cycles of catalysis (a,b). TEM images of Fe_3O_4/SiO_2-NH_2-Pt catalysts newly prepared (c) and after three cycles of catalysis (d).

of reduction, the Pt catalysts were dramatically leached from the support (Figure 5d). This can be explained by two main factors. First, because of the amplification effect of multifunctional HPs, compared with Fe_3O_4/SiO_2-NH_2 (-NH_2, 0.93 mmol/g; Pt, 0.053 mmol/g), the content of functional groups for Fe_3O_4/SiO_2/HPG (-COOH, 2.61 mmol/g; Pt, 0.296 mmol/g) is so high that more Pt^{2+} can be complexed for further formation of Pt nanoparticles. Second, the unique molecular structure of HPG is more helpful to tightly anchor the Pt catalysts compared with short amino-silane chains. Considering two amino groups are needed for complexing Pt^{2+}, the participant of functional groups for Fe_3O_4/SiO_2-NH_2 is 11%, which is even less than half of the value of Fe_3O_4/SiO_2/HPG (23%). Therefore, we can conclude that the HPG-tailored magnetic hybrids can be used as a versatile support to not only directly grow ultrasmall metal nanocatalysts on its surface but also well stabilize the nanocatalysts during the catalytic reaction.

To ascertain that other magnetic nanocatalysts are also highly reactive, the Fe_3O_4/SiO_2/HPG-Au and Fe_3O_4/SiO_2/HPG-Pd were examined by alcohol oxidation reaction and Heck reaction, respectively.

During the past decades, gold nanoparticles have been widely used as catalysts for a number of heterogeneous reactions such as hydrogenation, CO oxidation, and oxidation of alcohols.[40−42] The aerobic oxidation of alcohols over highly active immobilized catalysts with facile recyclable property is one of the most important and challenging reactions in organic synthesis and green chemistry. Herein the aerobic oxidation of alcohols was performed under air condition at room temperature using Fe_3O_4/SiO_2/HPG-Au as the catalyst. We first investigated the catalytic activities of Fe_3O_4/SiO_2/HPG-Au toward alcohol oxidation of the secondary alcohol 1-phenylethyl alcohol. After the reaction for only 2 h, the product (acetophenone) yield can reach as high as

Table 1. Results from Aerobic Oxidation of Benzylic Alcohol and 1-Phenylethyl Alcohol Catalyzed by Fe_3O_4/SiO_2/HPG-Au (Au Nanocatalysts)

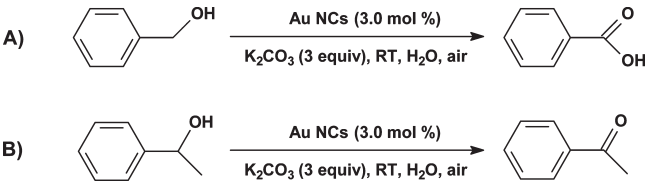

			product yield (%)			
entry	reaction	t (h)	1[b]	2[b]	3[b]	4[b]
1	A	2	78			
2[a]	A	6	89	88	88	87
3	B	2	95			
4	B	6	99	99	99	98

[a] Benzyl benzoate was additionally formed in 3% yield. [b] The cycle of reaction.

95%, and 99% of yield can be readily gained in 6 h (Table 1). The yield changes very little with longer time, hence 6 h was chosen as the time for each of this reaction. After the reaction, the catalyst was recovered by simple magnetic attraction, followed by washing with organic solvent and water to remove the organic reagents and K_2CO_3, and then reused for another batch of reaction. To our delight, the catalytic activity was maintained at least until the fourth use, with the oxidation occurring almost quantitatively (> 98%) in each run. In addition, the oxidation of the primary alcohol of benzyl alcohol was also examined. The product (benzoic acid) yields at 2 and 6 h reach 78% and 89%, respectively, which approaches or even exceeds the previously reported value by conducting the catalytic oxidation under an oxygen atmosphere at high temperature (100 °C).[43,44] Meanwhile, around 3% of benzyl benzoate derived from the reaction between benzoic acid and benzyl alcohol was formed. Similarly, the Au catalysts could maintain catalytic activity for at least four times of consecutive reaction. Thus, the Fe_3O_4/SiO_2/HPG-Au catalysts reported here not only possess the characteristic of facile magnetic separation but also show high catalytic activity for alcohol oxidation.

Heck reaction as a Pd-catalyzed carbon−carbon bond formation between aryl halides and olefins has occupied a special place in both common and state-of-the-art organic synthesis.[45,46] Conventional Heck reaction was performed in the existence of Pd catalyst and phosphine ligand that stabilizes the palladium during the reaction. Recently, more and more attention was focused on the development of a phosphine-free system for Heck reaction because the phosphines are usually toxic and expensive. So herein, we directly used Fe_3O_4/SiO_2/HPG-Pd as a catalyst for Heck reaction at 140 °C in DMF. The Heck cross coupling of two typical aryl halides of bromobenzene and iodobenzene with two representative olefins of aryl acid and styrene were studied, respectively (Table 2). It is found that the Fe_3O_4/SiO_2/HPG-Pd displayed higher catalytic activity compared to the previous report using Fe_3O_4/SiO_2-NH_2-Pd as a catalyst.[17] In addition, as is the usually case, the iodoaromatic is a more active substrate than the bromoaromatic, and styrene is more reactive than acryl acid. The feasibility of repeated use of Fe_3O_4/SiO_2/HPG-Pd was

(40) Corma, A.; Serna, P. *Science* **2006**, *313*, 332–334.
(41) Lopez, N.; Janssens, T. V. W.; Clausen, B. S.; Xu, Y.; Mavrikakis, M.; Bligaard, T.; Norskov, J. K. *J. Catal.* **2004**, *223*, 232–235.
(42) Kanaoka, S.; Yagi, N.; Fukuyama, Y.; Aoshima, S.; Tsunoyama, H.; Tsukuda, T.; Sakurai, H. *J. Am. Chem. Soc.* **2007**, *129*, 12060–12061.
(43) Kim, S.; Bae, S. W.; Lee, J. S.; Park, J. *Tetrahedron* **2009**, *65*, 1461–1466.
(44) Yang, X. M.; Wang, X. N.; Liang, C. H.; Su, W. G.; Wang, C.; Feng, Z. C.; Li, C.; Qiu, J. S. *Catal. Commun.* **2008**, *9*, 2278–2281.
(45) Beletskaya, I. P.; Cheprakov, A. V. *Chem. Rev.* **2000**, *100*, 3009–3066.
(46) Zhang, J. Z.; Zhang, W. Q.; Wang, Y.; Zhang, M .C. *Adv. Synth. Catal.* **2008**, *350*, 2065–2076.

Table 2. Results from Heck Reactions Catalyzed by Fe_3O_4/SiO_2/HPG-Pd (Pd Nanocatalysts)

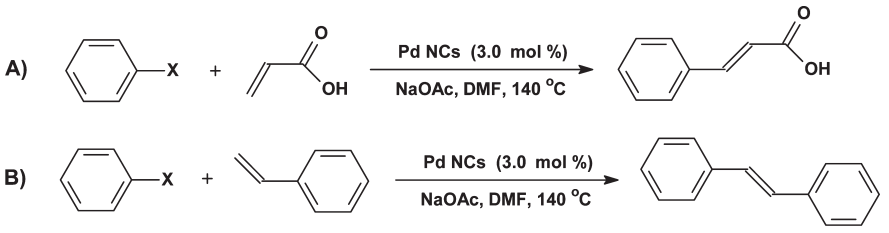

				product yield (%)			
entry	reaction	X	t (h)	1[a]	2[a]	3[a]	4[a]
1	A	Br	12	67	66	66	63
2	A	I	6	75			
3	A	I	12	81	81	80	78
4	B	Br	12	91	91	90	88
5	B	I	6	93			
6	B	I	12	97	97	96	95

[a] The cycle of reaction.

also examined. We present results from the investigation of recycling of Fe_3O_4/SiO_2/HPG-Pd for four successive reactions. No significant loss of catalytic activity was observed. For the reported fascinating PAMAM-Pd catalyst, however, the catalytic activity became lower and lower and even was completely lost after only three cycles of reaction due to the gradual thermal degradation of PAMAM templates under 140 °C, which resulted in leaching and aggregating of Pd nanoparticles.[24] Herein, because the HPG is highly stable below 200 °C and has been anchored on the surface of Fe_3O_4/SiO_2, the onset of the decomposition of temperature according to the TGA curves is 250 °C (Figure 2b) which is much higher than the reaction temperature (140 °C). Therefore, our Fe_3O_4/SiO_2/HPG-Pd is a quite promising catalyst for Heck reaction.

All of the above catalysis results demonstrate that the grafted-HPGs on the magnetic surfaces play the roles of both functional amplifier for high loading of nanocatalysts and stabilizer in the repeated use.

Conclusions

We developed a novel kind of robust magnetic hybrids based on the hyperbranched polyglycerol-functionalized Fe_3O_4/SiO_2 and used it as noble metal nanocatalyst supports for the first time. The HPG was directly grafted from the Fe_3O_4/SiO_2 by surface-initiated ring-opening polymerization of glycidol. Because of the unique structure and numerous functional groups of HPG, various noble metal nanocatalysts such as Pt, Au, and Pd could be directly grown on the surface of magnetic hybrids firmly with ultrasmall and monodisperse size, uniform distribution, and high loading capacity. Additionally, bifunctional hybrids with both fluorescent and magnetic properties could be facilely obtained by the conjugation of rhodamine B dye onto HPG. Reduction of 4-nitrophenol, alcohol oxidation, and Heck reaction were examined for the magnetic hybrid-supported Pt, Au, and Pd nanocatalysts, respectively. High catalytic activity was found for all the nanocatalysts, and moreover the noble metal nanocatalyst on the magnetic support has a very low leaching loss and can be reused at least three times without deactivation of catalytic activity. Conveniently, the noble metal nanocatalysts can be readily recycled by an external magnet because of their magnetic support. It is believed that this robust and facilely available magnetic nanohybrid will find promising applications in large-scale catalytic reactions in the industries. In addition, this robust magnetic support can also be utilized as a highly efficient adsorbent for metal ions, dyes, and proteins, and thus it will also find important applications in environment technology and biotechnology. All these studies will be reported elsewhere soon.

Acknowledgment. This work was financially supported by the National Natural Science Foundation of China (Grant No. 50773038 and Grant No. 20974093), National Basic Research Program of China (973 Program, Grant No. 2007CB936000), Science Foundation of Chinese University, and the Foundation for the Author of National Excellent Doctoral Dissertation of China (Grant No. 200527).

Supporting Information Available: Magnetization curve of Fe_3O_4, TGA curve of Fe_3O_4/SiO_2-NH_2, more TEM images of Fe_3O_4/SiO_2/HPG-Pt, Fe_3O_4/SiO_2/HPG-Au, and Fe_3O_4/SiO_2/HPG-Pd, SEM images of Fe_3O_4/SiO_2/HPG-Au and Fe_3O_4/SiO_2/HPG-Pd, and their corresponding EDX spectra. This material is available free of charge via the Internet at http://pubs.acs.org.